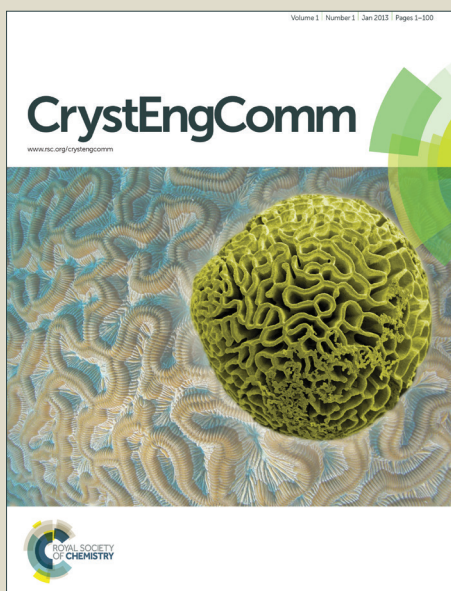


CrystEngComm

Accepted Manuscript



This is an *Accepted Manuscript*, which has been through the Royal Society of Chemistry peer review process and has been accepted for publication.

Accepted Manuscripts are published online shortly after acceptance, before technical editing, formatting and proof reading. Using this free service, authors can make their results available to the community, in citable form, before we publish the edited article. We will replace this *Accepted Manuscript* with the edited and formatted *Advance Article* as soon as it is available.

You can find more information about *Accepted Manuscripts* in the [Information for Authors](#).

Please note that technical editing may introduce minor changes to the text and/or graphics, which may alter content. The journal's standard [Terms & Conditions](#) and the [Ethical guidelines](#) still apply. In no event shall the Royal Society of Chemistry be held responsible for any errors or omissions in this *Accepted Manuscript* or any consequences arising from the use of any information it contains.

Cite this: DOI: 10.1039/c0xx00000x

www.rsc.org/xxxxxx

ARTICLE TYPE

Auxiliary ligand aided tuning of aggregation in transition metal benzoates: Isolation of four different types of coordination polymers†

Subarna Banerjee,^a Palanisamy Rajakannu,^a Raymond. J. Butcher,^b and Ramaswamy Murugavel^{a,*}

Received (in XXX, XXX) Xth XXXXXXXXX 200X, Accepted Xth XXXXXXXXX 200X

DOI: 10.1039/b000000x

Reactions of alkyl substituted aromatic mono carboxylic acids with first row transition metal ions in the presence of chelating and bridging N,N-donor ligands produce a variety of discrete and polymeric complexes, depending on the position of the substituent on benzoic acid and the ability of auxiliary ligand to act as a chelating or bridging ligand. Ten different compounds isolated in the present study fall into two different structural types, viz. discrete mono or/ dinuclear complexes ($[\text{Cu}(\text{L}^1)_2(\text{AL}^1)(\text{H}_2\text{O})]$ (**1**), $[\text{Mn}(\text{L}^1)_2(\text{AL}^1)_2]$ (**2**) and $[\text{Zn}(\text{L}^1)_2(\text{AL}^1)_2]$ (**3**) and polymeric compounds (**4-11**). The polymeric compounds isolated can further be classified into four different structural types, viz. 1-D helical polymers, linear 1-D polymeric chains, rail-road like polymers and 2-D polymeric sheets. The structure modulation is a result of combination of the types of substituents on the aryl ring of the benzoic acid and the nature of the auxiliary ligand used. For example, when 1,10-phenanthroline used as the auxiliary ligands, if the carboxylic acid used is 4-tert-butyl benzoic acid, discrete complexes have been isolated. However, for the same auxiliary ligand when 2,4,6-trimethyl benzoic acid is used as the carboxylate, a series of 1-D helical polymers ($[\text{M}(\text{L}^2)_2(\text{AL}^1)(\text{H}_2\text{O})]_n$ M = Mn (**4**); Co (**5**); Cu (**6**); Zn (**7**)) have been obtained. This clearly demonstrates the ability of o,o'-disubstituted benzoic acids to form helical polymers, whereas p-substitution on the aryl ring results in discrete complexes. The reactions of metal acetates with benzoic acid in the presence of 4,4'-bipyridine has been found to be sensitive to the ortho substituents on the acid. When two equivalents of 2,4,6-triisopropyl benzoic acid was used, a linear polymer ($[\text{Zn}(\text{L}^3)_2(\text{AL}^2)]_n$ (**8**)) is obtained. The use of either one or two equivalents of 2,4,6-trimethyl benzoic acid invariably leads to the isolation of rail-road like polymers ($[\text{M}(\text{L}^2)(\text{OAc})(\text{AL}^2)]_n$ M = Mn (**9**) and Zn (**10**)) where the rails are bridged by acetate ligand. Replacing the carboxylic acid by a phosphate diester leads to the isolation of a 2-D polymer ($[\text{Zn}(\text{L}^4)_2(\text{AL}^2)]_n$ (**11**)), due to the ability of phosphate to act exclusively as a bridging ligand. In addition to extensive analytical and spectroscopic characterization of the products, the solid-state structures of all the new compounds have been determined using single crystal X-ray diffraction.

Introduction

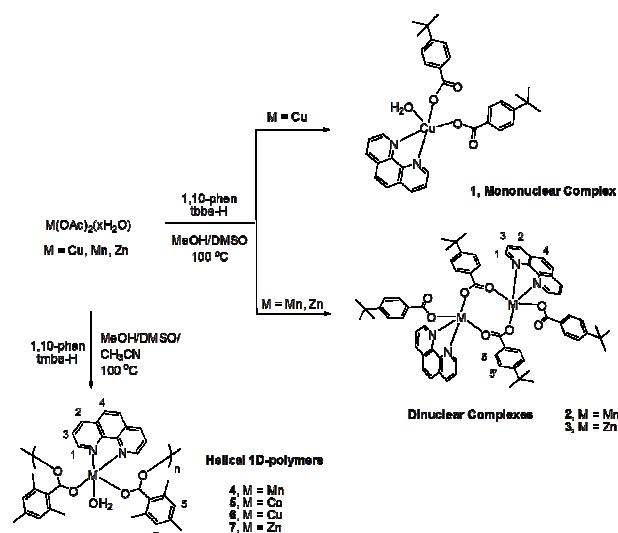
Inorganic-organic hybrid materials are accessible today through rational synthesis using a wide choice of metal ions and an infinite choice and design of ligands.¹⁻² Metal carboxylates are very much in vogue in recent years for the preparation of hybrid metal-organic frameworks.³⁻⁵ Although quite a number of compounds have been synthesized containing mono carboxylic acids and many structurally characterized compounds in this class are known, there is little information in the literature on studies where systematic efforts have been made to fully understand the structural aspects and binding preferences of mono carboxylic acid complexes in the context of frameworks solids.⁶⁻⁷ The introduction of ancillary ligand 1,10-phenanthroline (1,10-phen, AL¹) and 4,4'-bipyridine (4,4'-bpy, AL²) which have different ligation behavior may induce new structural evolution leading to complexes with tunable dimensions and physical properties.⁶⁻⁹ The dimensions of the desired compounds can be varied by using the length of the linker or the bulky substituents on the phenyl ring of the aryl carboxylate organic building units.¹⁰ The geometry of the resultant architectures depend on several factors such as coordination geometry of the metal ion, presence of guest molecules, ligand and transition metal ratio and the type and

shape of anions.¹¹ The ligand 4,4'-bipyridine is an ideal connector between the transition metal atoms for the propagation of coordination networks¹² and an excellent bridging ligand giving rise to a large number of one-, two-, and three-dimensional frameworks with grids and channels. In addition, hydrogen bonding gives rise to attractive, multi-directional and selective properties of the compounds obtained thereby.¹³⁻¹⁴ In the present work, we have chosen three simple organic building units, 4-tert-butylbenzoic acid (L¹H, tbbaH), 2,4,6-trimethylbenzoic acid (L²H, tmbaH) and 2,4,6-triisopropylbenzoic acid (L³H, tipbaH) and various metal acetate salts with two different types of auxiliary ligands (one chelating and one bridging N-N-donors) as starting materials to address the objective of tuning coordination geometry and aggregation behavior of resultant products. The results of these investigations are described herein.

Results and discussion

A. Role of chelating unit in the reaction of transition metal benzoates with substituted benzoic acids. Complexes **1-6** have been synthesized from a reaction of metal acetates (M = Mn, Cu and Zn) with AL¹ and substituted benzoic acids (L¹H/L²H) in methanol and DMSO/acetonitrile (Scheme 1). The resulting

single crystals of metal benzoate complexes are air- and moisture stable and are soluble in organic polar solvents such as DMSO.



Scheme 1 Synthesis of discrete and 1-D helical polymeric complexes 1-7.

The FT-IR spectra of complexes show strong absorption bands at around 2960 and 2875 cm^{-1} , that are due to the C-H vibrations of the *tert*-butyl group of the acid in 1-3. Complexes 1 and 4-7 show a band at around 3368 cm^{-1} due to O-H stretching vibration of water or methanol. The $\nu_{\text{as}}(\text{COO}^-)$ is observed at 1636 cm^{-1} while $\nu_{\text{s}}(\text{COO}^-)$ is observed at around 1431 cm^{-1} . The ^1H NMR spectrum of complex 3 in $\text{dms}\text{-}d_6$ shows well separated peaks for all the protons of AL^1 and L^1 ligands. The peaks in the range 8.13-8.92 ppm correspond to the aromatic protons H^{1-4} of AL^1 ligand (Fig.1). The downfield shift of protons H^1 - H^4 of AL^1 ligand compared to free AL^1 is consistent with the loss of electron density after coordination to the metal ion. Two doublets appear at 7.82 and 7.35 ppm for arene protons of L^1 . The methyl-protons of *tert*-butyl group appear as singlet at δ 1.24 ppm. Similarly, compound 7 also shows well separated peaks in the range 8.31-9.25 ppm and 7.42-7.84 ppm for all the aromatic protons of AL^1 and benzoic acid ligands, which are downfield shifted compared to free ligands. The ^{13}C NMR spectra of 3 and 7 show well separated peaks for all the carbon atoms in the molecule..

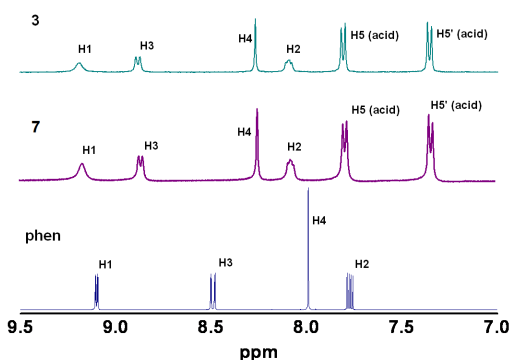


Fig. 1 ^1H NMR spectra of 3 (top) and 7 (middle) and free 1,10-phen (bottom) in $\text{DMSO-}d_6$.

The ESI-MS spectrum of 1 shows a peak at m/z 600.165 corresponding to the $1\text{-H}_2\text{O}$ ion. This indicates that under mass spectral conditions water molecule is removed from the complex in solution to give $[\text{Cu}(\text{L}^1)_2(\text{AL}^1)]$. Compounds 2 and 3 exhibit ions at m/z 592.175 and 601.168, respectively, due to the monomeric form $[\text{M}(\text{L}^1)_2(\text{AL}^1)]$ formed under mass spectral conditions. The ^{13}C NMR and ESI-MS spectra are included in supporting information (Fig. S1-S5).

Molecular structure of discrete complexes. The reaction of metal acetate with AL^1 and substituted benzoic acid can in principle provide two types of complexes viz. either discrete or polymeric systems. Since 1,10-phenanthroline (AL^1) is known only to chelate metal ion, it is generally believed that in presence of AL^1 only discrete complexes are expected to result. The carboxylate ligand on the other hand either can act as chelating or bridging ligand apart from the possibility of acting as terminal monodentate ligands with free C=O group under unfavorable chelating or bridging condition (Fig. 2). Hence in order to unravel, the coordination behavior of L^1 and L^2 in the presence of AL^1 , compounds 1-7 have been probed by single crystal X-ray diffraction.

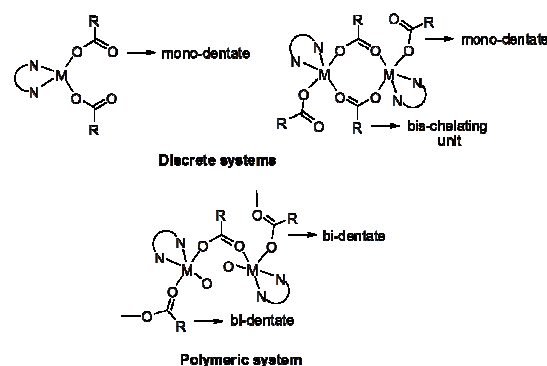


Fig. 2 Aggregation of transition metal benzoates (from discrete to polymeric system).

Structure of mononuclear complex $[\text{Cu}(\text{L}^1)_2(\text{AL}^1)(\text{H}_2\text{O})](\text{H}_2\text{O})$ (1). Compound 1 crystallizes in the triclinic space group $\text{P}\bar{1}$. In $[\text{Cu}(\text{L}^1)_2(\text{AL}^1)(\text{H}_2\text{O})]$ (1), the central metal ion is coordinated to one 1,10-phen, two acids and one water molecule (Fig. 3). The acid acts as a monodentate ligand. This is reflected in the C-O bond distances. The coordinated oxygen of tbbz has a longer bond length {O(1)-C(1): 1.279(4) Å} than the non-coordinated oxygen (O(2)-C(1): 1.231(4) Å).

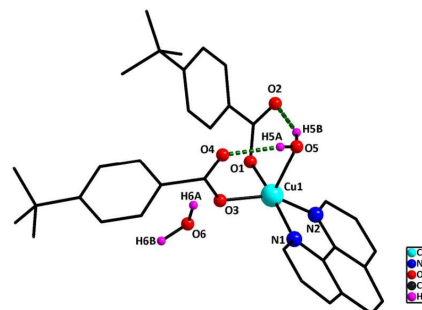


Fig. 3 Molecular structure of $[\text{Mn}(\text{L}^1)_2(\text{AL}^1)(\text{H}_2\text{O})](\text{H}_2\text{O})$ (1).

The central copper ion adopts a distorted square pyramidal environment with two nitrogen atoms from 1,10-phen, two oxygen atoms from tbba acid and one oxygen from the coordinated water molecule surrounding the metal ion. There are intramolecular H-bonding interactions between the hydrogen atoms of the coordinated water molecule and the oxygen atoms of the acid molecules (O5-H5A...O4: 2.0609(5) and O5-H5A...O2: 1.919(6) Å), apart from the intermolecular H-bonding interactions between the hydrogen atoms of the free uncoordinated water molecule and the oxygen atoms of the acid molecules (O6-H6b...O2: 1.896(5) and O6-H6b...O3: 2.509(4) Å). These secondary interactions lead to the formation of a 1-dimensional polymer as shown in Fig. 4. Selected bond lengths and angles in **1** are given in Table S1. The comparison of parameters of **1** with related Cu-phen complexes is presented in Table S2.¹⁷

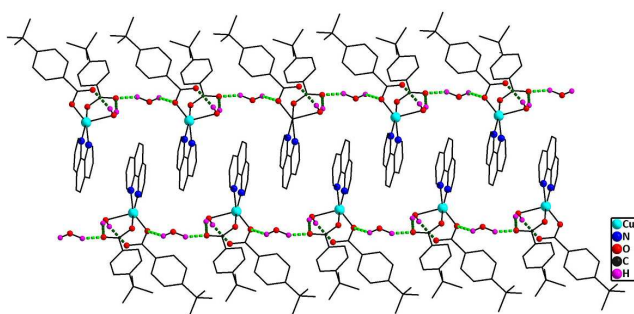


Fig. 4 Inter/intra-molecular hydrogen bonding interactions in **1**.

Structure of $[M(L^1)_2(AL^1)_2](2CH_3OH)$ (2**, $M = Mn$; **3**, $M = Zn$).** Yellow crystals of **2** and colorless crystals of **3** were obtained

from the respective reaction mixture (methanol and DMSO). Compound **2** crystallizes in the monoclinic $C2/c$ space group. Crystal structure of **2** contains two manganese ions, four tbba acids and two 1,10-phen units apart from two methanol solvent molecules are present in the crystal lattice. The Mn^{2+} ions adopt distorted square pyramidal geometry with $-N_2O_3$ coordination environments as shown in Fig. 5. Each manganese ion is coordinated by two nitrogen centers of 1,10-phen unit, one oxygen of a tbba unit in monodentate mode and two oxygen atoms of bidentate two tbba units. Among the four tbba acids, two act as monodentate and other two act as bis-chelating ligand and bridge two Mn^{2+} ions, thus forming eight-membered ring. The C-O bond distances observed in the carboxylate group units also support the fact that the acid coordinates either in a bidentate or monodentate fashion. The two 1,10-phen units are tightly packed and are held together through π - π interactions. The carbon atoms of one of the 1,10-phen units exhibit π - π interactions with the centroid of the arene unit of another 1,10-phen at a distance of around 3.924(2) Å as shown in Fig. 5 and Fig. S6. The arrangement of four tbba units around the two metal ions shows resemblance to a bowl. The 1,10-phen unit of adjacent molecules sit on the bowl through hydrogen bonding interactions between hydrogen atoms of 1,10-phen unit and oxygen atoms of tbba units (O3...H17: 2.854(2) Å and O4...H18: 2.626(4) Å) leading to the formation of a 1-dimensional polymeric structure. Selected bond lengths and angles for **2** are listed in Table S3. A comparison of structural parameters of **2** with related Mn-phen complexes is presented in Table S4.¹⁸

Compound **3** is isomorphous to compound **2** and crystallize in the monoclinic $C2/c$ space group (Fig. 5). Selected bond lengths and angles in **3** are listed in Table S5 and a comparison of parameters with related known Zn-phen complexes is presented in Table

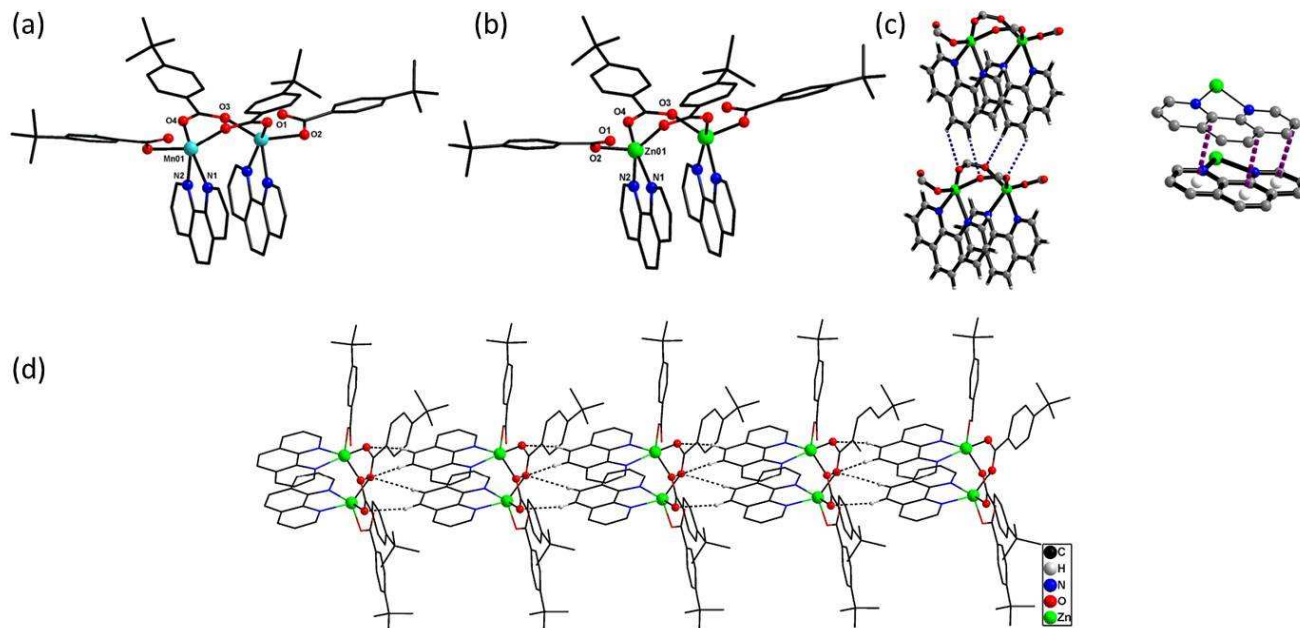


Fig. 5 Molecular structure of $[Mn_2(L^1)_4(AL^1)_2](2CH_3OH)$ (**2**) (a) and $[Zn_2(L^1)_4(AL^1)_2](2CH_3OH)$ (**3**) (b) (hydrogen atoms and solvent molecules are omitted for clarity), CH- π and π - π interactions in **2** (c) and Formation of a 1-dimensional polymer through intermolecular hydrogen bonding interactions between adjacent molecules of phen and tbba ligands in **3**.

S6.¹⁹ Like in **2**, the arrangements of four tbba units resemble to one big bowl and 1,10-phen unit of adjacent molecule sits on the bowl through hydrogen bonding interactions (O3...H26A: 2.757(5) Å and O4...H27A: 2.580(4) Å) which results in the formation of a 1-dimensional polymer (Fig. 5).

Molecular structure of 1-D helical polymers

$[M(L^2)_2(AL^1)(H_2O)]_n$ (**4-7**) ($M = Mn, Co, Cu, Zn$). Single crystal X-ray diffraction studies reveal that compounds **4-7** are isomorphous, which crystallize in tetragonal $I4_1$ space group (Fig. 6). Selected bond distances and angles are listed in Table S7. Crystal structure of **4** contains a manganese ion bound to one 1,10-phen, two L^2 and one water molecule. The central manganese ion is hexa-coordinated with a distorted octahedral geometry. Two nitrogen centers of 1,10-phenanthroline, two oxygen atoms of two different tmba acids and one oxygen of water account for five coordination sites at the metal. The oxygen from another carboxylate (that is bridging to manganese) satisfies the sixth coordination site. The tmba ligand acts as a bridging unit to two Mn(II) atoms via its carboxylate oxygen atoms.

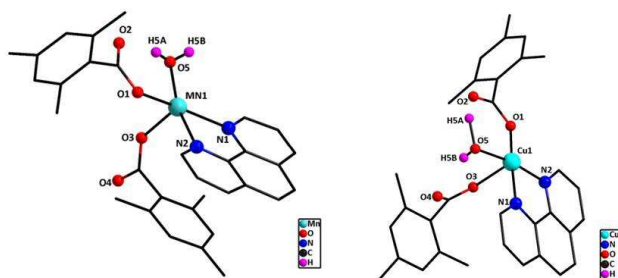


Fig. 6 Molecular structures of the asymmetric part (repeating unit) of $[Mn(L^2)_2(AL^1)(H_2O)]_n$ (**4**) (left) and $[Cu(L^2)_2(AL^1)(H_2O)]_n$ (**6**) (right).

The Mn-O (carboxylate) distances are not equal; Mn(1)-O(3): 2.189(1) Å is longer than Mn(1)-O(1): 2.099(1) Å. The Mn-O (water) distance is the longest (2.220(1) Å). The average Mn-O-C angle is 131.255°. As a consequence of the tmba bridge, compound **4** has an extended 1-D helical structure as shown in Fig. 7.

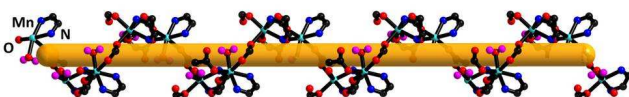


Fig. 7 Helical structure of $[Mn(L^2)_2(AL^1)(H_2O)]_n$ (**4**).

Each $[Mn(L^2)_2]_n$ in the 1-D chain is linked through hydrogen bonds to three neighboring chains having opposite helicity with a Mn...Mn distance of 5.591(1) Å. The water hydrogen atoms are involved in hydrogen bonding with the carboxylate oxygen of the neighboring chains. Moreover, 1-D helical network has hydrogen-bonded sites oriented in three directions, leading to a 3-D network having small channels. Therefore the water molecule allows the construction of molecular frameworks in which the infinite 1-D helical building units are linked to form 3-D

hydrogen bonded network. The formation of an infinite chain the complex rather than a simple mononuclear complex or any other motif is attributed to the steric hindrance provided by the bulky *o,o'*-dialkyl substitution of the aryl ring. Comparison of the structural parameters of previously reported Mn(II)-carboxylate complexes having -O and -N coordination core with 1,10-phen ligand, with compound those of **4** is presented in Table S4.¹⁸

Compound **5** is isomorphous to **4** and hence also forms a helical structure (Fig. S7). The Co-O (carboxylate) distances in the molecule are not equal (Co(1)-O(3): 2.167(2) Å is longer than Co(1)-O(1): 2.044(2) Å). The Co-O (water) distance (2.145(2) Å) is similar to Cu-O (carboxylate) bonds. The average Co-O-C angle is about 131.02°. Compound **6** is also isomorphous to compounds **4** and **5**, and hence it also forms a helical structure and crystallizes in the tetragonal crystal system with space group $I4_1$ (Fig. 6). The Cu-O (carboxylate) distances in the molecule are not equal (Cu(1)-O(3): 2.405(5) Å is longer than Cu(1)-O(1): 1.947(5) Å). The Cu-O (water) distance (2.005(5) Å) is the longest among Cu-O bonds in **5**.¹⁹ The average Cu-O-C angle is about 125.9°. In the O_2N_2 basal plane of **5**, the O(1)-Cu(1)-N(1) and O(1)-Cu(1)-N(2) angles are 170.7(2)° and 89.8(2)°, respectively. The average cis-angle around copper ion is 89.5(2)° (Table S8). A literature compilation of copper-1,10-phen complexes where the central metal ion Cu(II) is having -O and -N coordination is given in Table S2.¹⁷ Compound **7** is also isostructural to compounds **4-6**, having the same crystal parameters with the formula $[Zn(L^2)_2(AL^1)(H_2O)]_n$. However, the full structural solution is not possible in this case due to persistent twinning problems. The *c*-axis gets tripled and thus there are three zinc atoms and associated ligands in the asymmetric unit of **6** (Fig. S7). A comparison of zinc-1,10-phenanthroline complexes with -O and -N coordination is presented in Table S6.¹⁹

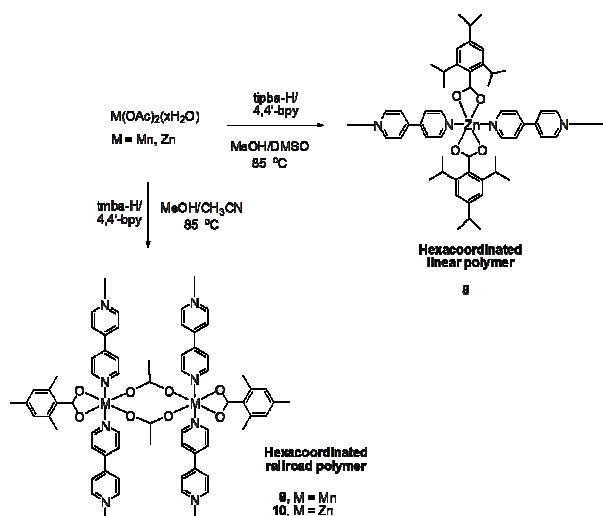
The description of structures of **1-7** described above clearly show that the aggregation of metal benzoates are tuned from mononuclear complex to helical polymers through discrete dinuclear systems by using different substituted benzoic acids. The ortho-methyl substituted acid aids the formation of helical polymers while the para-*tert*-butyl group substituted benzoic acid leads to isolation of discrete systems because of steric reasons. The formation of monomeric form in **1** may be ascribed to the preference of copper ions to form square pyramidal geometry over the *tbp* geometry observed for Zn and Mn metal ions in complexes **2** and **3**.

B. Role of linear ditopic N-donors in the reaction of transition metal benzoates with substituted benzoic acids

Ditopic spacers such as 4,4'-bipyridine, where the two donor sites are diagonally opposite to each other have been extensively used as building blocks to build linear to 3-D structures when suitable metal ions are used in conjunction with other ligands such as carboxylic acids. In spite of the richness of the chemistry of 4,4'-bipyridine as a spacer ligand,¹² surprisingly there are not many reports in the literature where bulky mono carboxylic acids have been used in conjunction with 4,4'-bipyridine to build coordination polymers.

Reactions of AL^2 with manganese and zinc acetate with substituted benzoic acids (L^2H/L^3H) in methanol and DMSO lead

to formation of complexes **8-10** (Scheme 2). The resultant single crystals of metal benzoates complexes obtained are air- and moisture stable and soluble in organic polar solvents. The ^1H NMR spectrum of **8** shows well separated peaks for all the protons of AL^2 and L^3 ligands with a 1:2 intensity ratio. The two doublets appearing at 8.75 and 7.88 ppm correspond to the $4,4'$ -bpy protons and the singlet observed at 6.93 ppm is due to the arene protons of the tipba unit. Complex **10** also shows well separated resonances for AL^2 and L^2 unit protons with 1:1 ratio as shown in Fig. S8. The ^{13}C NMR spectra are included in supporting information (Fig. S9-S12).



Scheme 2 Synthesis of polymers **8-10** using AL^2 with metal acetates and substituted benzoic acids.

Molecular structure of hexa-coordinated linear polymer $[\text{Zn}(\text{L}^3)_2(\text{AL}^2)]_n$ (8**).** A single crystal X-ray diffraction study has been carried out for compound **8** in order to establish its solid-state structure. The compound crystallizes in the monoclinic space group C2/m . The asymmetric unit of the unit cell of **7** reveals that the central metal zinc ion is coordinated to one end of two $4,4'$ -bpy ligands and two tipba acid molecules (Fig. 8). The geometry around zinc can be best described as distorted octahedral with O_4N_2 coordination environment.

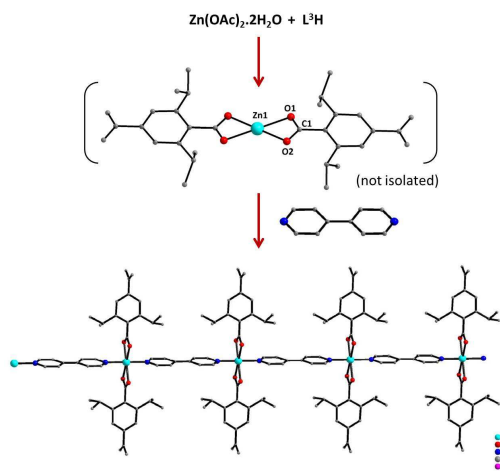


Fig. 8 Possible structure evolution of 1-D linear polymeric chain

in $[\text{Zn}(\text{L}^3)_2(\text{AL}^2)]_n$ (**8**) (hydrogen atoms are omitted for clarity).

The six coordination sites of the metal are satisfied by four oxygen atoms of two acids and one nitrogen atoms of two $4,4'$ -bpy unit, thus leading to the formation of a linear 1-D polymer as shown in Fig. 8. The sterically crowded carboxylic acid (L^3) acts a bidentate chelating ligand and having similar O-C distances ($\text{O}(1)-\text{C}(1)$: 1.265(4) Å; $\text{O}(2)-\text{C}(1)$: 1.260(4) Å) (Table S9). In addition there are hydrogen bonding interactions between oxygen atoms of L^3 and hydrogen atoms of AL^2 ($\text{O}1 \cdots \text{H}22-\text{C}22$: 2.566(2) Å) which leads to the formation of 2-D sheet as depicted in Fig. 9. Comparison of previously reported some zinc- $4,4'$ -bpy complexes with **8** are presented in Table S10.²⁰

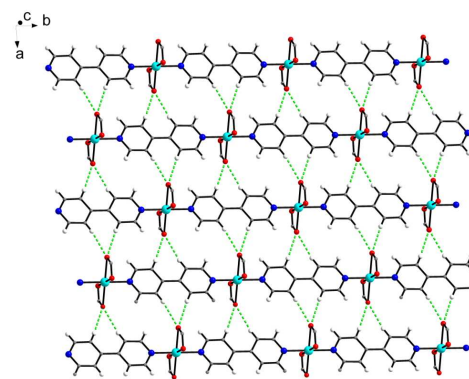


Fig. 9 2-D sheet formation in **8** through C-H \cdots O hydrogen bonding interaction (triisopropylbenzene units omitted for clarity).

Molecular structure of hexa-coordinated rail-road polymers **9** and **10**

$[\text{M}(\text{OAc})(\text{L}^2)(\text{AL}^2)]_n$ (**9**, $M = \text{Mn}$; **10**, $M = \text{Zn}$). Crystals of **9** and **10** suitable for X-ray measurement were obtained from the reaction mixture in methanol/DMSO mixture after 5 days. Compound **9** crystallizes in monoclinic $\text{P2}_1/\text{c}$ space group. The basic structural motif of **9** is shown in Fig. 10. Here two manganese ions are bridged by two acetate ligands to produce an eight-membered $\text{M}_2\text{O}_4\text{C}_2$ metal carboxylate ring.

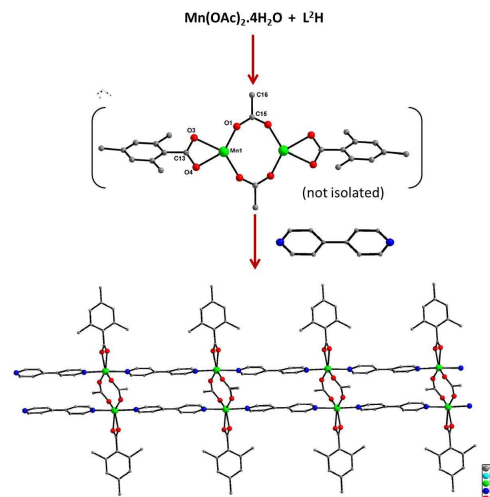


Fig. 10 Possible structure evolution in manganese polymer **9** $[\text{Mn}(\text{OAc})(\text{L}^2)(\text{AL}^2)]_n$.

Each of the metal ion is further chelated by a trimethyl benzoate (L^2) ligand, taking the coordination number around each divalent metal to form. The remaining two coordination sites on the metal is taken up by two bridging 4,4'-bpy ligands. By the ability of 4,4'-bpy ligand to bridge the adjacent $[M_2(\mu\text{-acetate})_2(L^2)_2]$ units as shown in Fig. 10, results in the formation of "rail-road" like polymer. The two nearest manganese ions across the two "rails" are separated from each other by 4.066(2) Å, which is roughly also distance between the two rails. The adjacent manganese ions along each of the rails are separated by 11.960(3) Å. Thus, these polymeric structures can be regarded as a highly periodic 1-D polymer made of two parallel metal chains with bridges between them through acetate anions. The two Mn-O(acetate) distances around the Mn ions are almost similar (Mn-O1: 2.103(2) Å; Mn-O2: 2.094(5) Å). The L^2 which act as the bidentate chelating ligand display the longer Mn-O(acid) distances (Mn-O3: 2.231(2) Å; Mn-O4: 2.297(5) Å). Other selected bond lengths and angles are listed in Table S11. The C-H...O hydrogen bonding interactions between oxygen atoms of L^2 and hydrogen atoms of AL^2 ($O4\cdots H7-C7$: 2.454 and $O4\cdots H2-C2$: 2.296 Å) which leads to the formation of 2-D sheets. A second hydrogen bonding between the uncoordinated methanol and oxygen atoms of L^2 ($O3\cdots H5A-O5$: 2.274 Å) has also been observed (Fig. 11).

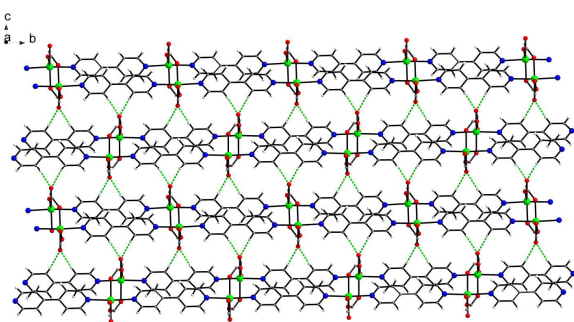
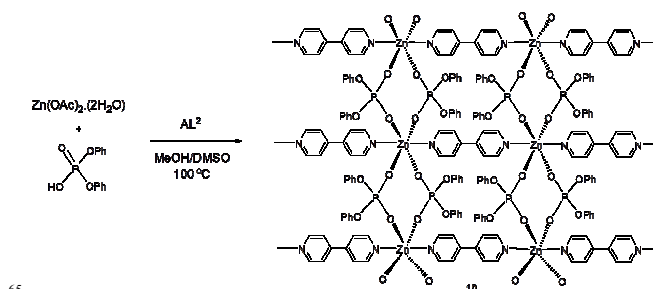


Fig. 11 2-D sheet formation through hydrogen bonding in **9**.

The two Mn-O(acetate) distances around the Mn ions are almost similar (Mn-O1: 2.103(2) Å; Mn-O2: 2.094(5) Å). The tmba which act as the bidentate chelating ligand display the longer Mn-O(acid) distances (Mn-O3: 2.231(2) Å; Mn-O4: 2.297(5) Å). Other selected bond lengths and angles are listed in Table S11. The C-H...O hydrogen bonding interactions between oxygen atoms of L^2 and hydrogen atoms of AL^2 ($O4\cdots H7-C7$: 2.454 and $O4\cdots H2-C2$: 2.296 Å) which leads to the formation of 2-D sheets. A second hydrogen bonding between the uncoordinated methanol and oxygen atoms of L^2 ($O3\cdots H5A-O5$: 2.274 Å) has also been observed (Fig. 11).

Compound **10** is isostructural to **9** and crystallizes in monoclinic $C2/c$ space group (Fig. S13 and S14). In addition to the contents of **9**, lattice DMSO solvents have been found to be present in **10**. The acetate group act as bridging unit and the Zn-O(acetate) distances are almost equal as in **9** (Zn-O3: 2.029(2) Å; Zn-O4: 2.025(3) Å). The bidentate chelating tmba acid Zn-O(acid) distances (Zn-O1: 2.450(2) Å; Zn-O2: 2.080(5) Å) show significant non equivalent of Zn-O distance unlike in **9**. Selected bond lengths and angles are listed in Table S12 and comparison of previously reported zinc-4,4'-bpy complexes to **10** is presented in Table S10.²⁰

C. Role of phosphate ligand in the formation coordination polymer. The molecular structure of **9** and **10** reveal the strong preference for HL^2 (substituted benzoic acids) to act exclusively as bidentate chelating ligands in the presence of 4,4'-bipyridine linkers. However it has been well established in the literature that phosphinic acids $R_2\text{POOH}$ and dialkyl/aryl phosphate (RO)POOH seldom involve in chelating mode of coordination but prefer the role of bridging ligand and connect two or more metal atoms. Hence, the sterically crowded benzoic acid was replaced with a diaryl phosphate in order to synthesize layered structure. The reaction of zinc acetate with 4,4'-bipyridine (AL^2) and diphenylphosphate (dppH) in methanol/DMSO mixture yields the coordination polymer **11** (Scheme 3), which is completely different from the rail-road like metal carboxylate based polymers **9** and **10**. Compound **11** has been characterized by analytical and spectroscopic methods.



Scheme 3 Synthesis of metallophosphate polymer **11** using AL^2 with metal acetates and L^4H .

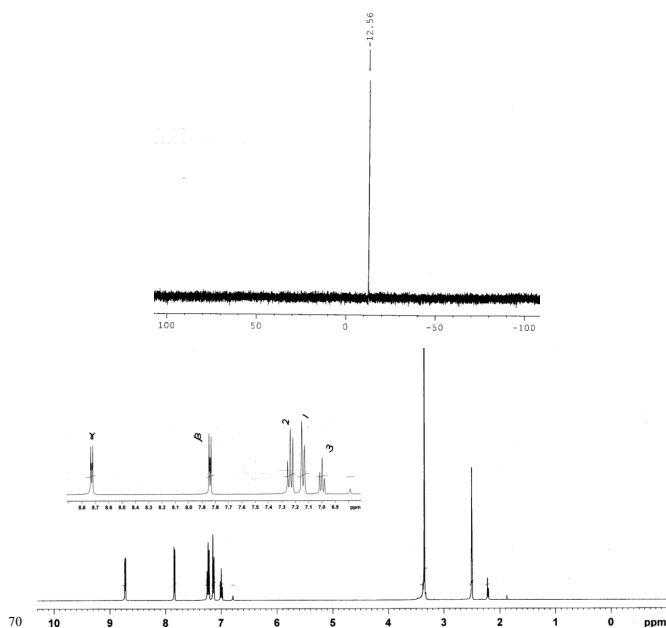


Fig. 12 ^{31}P (top) and ^1H NMR (bottom) spectra of **11** in $\text{DMSO-}d_6$.

The elemental analysis for polymer **11** is in well agreement with its solid-state structure. The FT-IR spectrum of **11** shows absorption bands at 2977, 1184 and 1069 cm^{-1} corresponding to the $\nu_{\text{asy}}(\text{C-H})$, $\nu_{(\text{P-O-O})}$ and $\nu_{\text{M-O-P}}$ vibrations. Absence of any

absorption in the range 2700-2500 cm^{-1} indicates that the neutralization of dppH ligand. The ^{31}P NMR spectrum of **11** shows a single resonance at -12.56 ppm indicating the presence of only one types phosphorus center in the product (Fig. 12). The ^1H NMR spectrum of **11** shows well separated peaks for all the protons of AL^2 and dpp ligand in a 1:2 ratio of the intensities. Two doublet of doublets have been observed at 8.73 and 7.84 ppm for the α and β protons of AL^2 units. Aromatic protons of dpp appear as two triplets (7.25 and 7.01 ppm) and a doublet (7.15 ppm) in the aromatic region (Fig. 12 and Fig. S15).

Molecular structure of $[\text{Zn}(\text{L}^4)_2(\text{AL}^2)]_n$ (11**).** Attempts to obtain single crystal suitable for diffraction studies always yielded poor quality non-transparent crystals with high degree of mosaicity. The best of these crystals were obtained from one batch of the reaction mixture after 1 week through slow evaporation. Compound **11** crystallize in monoclinic $C2/c$ space group. The central zinc ion adopts a slightly distorted octahedral arrangement with a $-\text{N}_2\text{O}_4$ coordination environment. Each metal ion is surrounded by four oxygen atoms from four different bridging dpp ligands and two nitrogen atoms of two different 4,4'-bpy ligands. The two N-atoms at the metal occupy the trans positions and thus facilitate the formation of 2-D sheet structure. The M-O(P) and M-N bond length (2.09(1)/2.11(1) Å and 2.10(2)/2.16(2) Å) are comparable with the previously reported complexes formed by dppH with Cu, Ca and Pb metal ions.²¹ The structure of **11** can be regarded as a two-dimensional sheet made of a linear 1-D polymer $[\text{Zn}(\text{dpp})_2]$ which is doubly bridged by two 4,4'-bipyridine ligands (Fig. 13).

Comparison of polymeric structures 4-11. Structure determination for compounds **4-11** revealed the fact that different types of 1-D coordination polymers can be assembled by engineering both primary (benzoic acid derivative) and auxiliary

(N,N' -donor) ligands. Although it is generally expected that the use of 1,10-phen donor should lead to formation of discrete metal complexes such as **1-3**, polymer formation can be easily induced

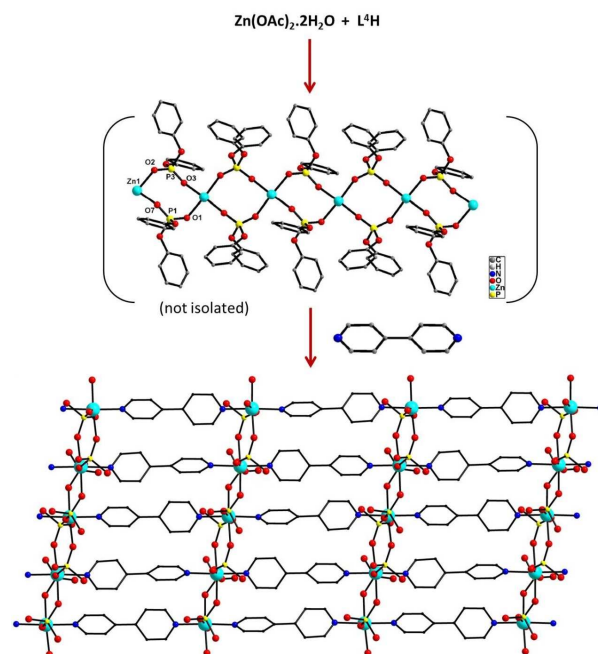
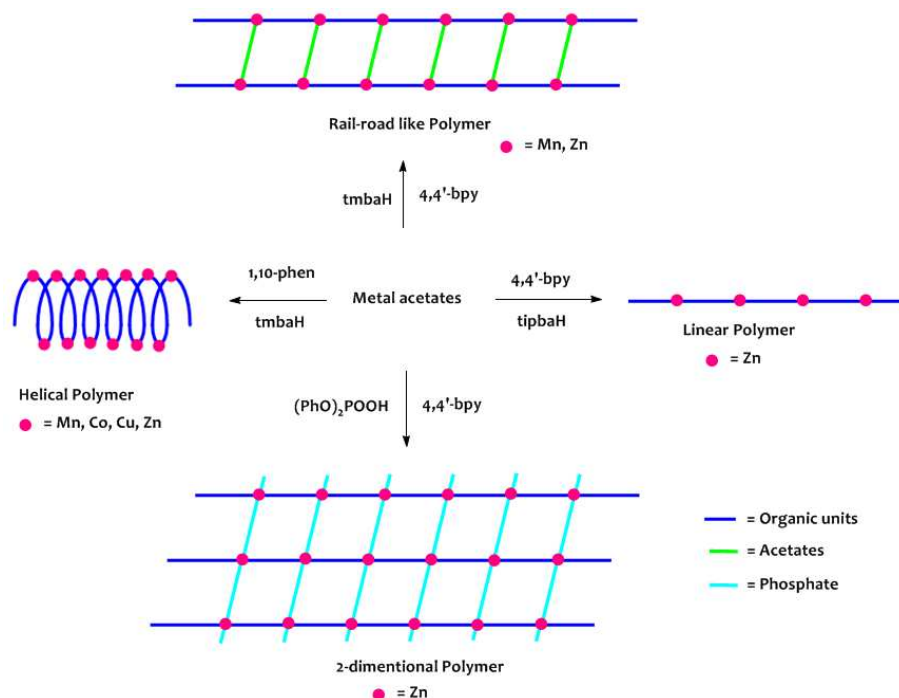


Fig. 13 Structure evolution of 2-D polymeric sheet in **11** (peripheral atoms are omitted for clarity).

by a simple substitution of alkyl groups at o,o' -positions of the benzoic acids. The bulky substituent at the vicinity of COO^- group tend to direct L^1H and L^2H to be predominantly bridging ligands and hence 1-D helical polymer can be exclusively isolated (path a; Scheme 4). However, when 4,4'-bipyridine is



Scheme 4 Comparison of polymeric structures **4-11**.

Table 1 Crystal data's for compounds 1-6 and 8-11.

Compound	1	2	3	4	5
Identification code	RM145a	RK1_141	RK1_139	SG	RK1-417
Formula	C ₃₄ H ₃₈ CuN ₂ O ₆	C ₇₀ H ₇₆ Mn ₂ N ₄ O ₁₀	C ₆₈ H ₇₆ N ₄ O ₁₂ Zn ₂	C ₃₂ H ₃₂ MnN ₂ O ₅	C ₃₂ H ₃₂ CoN ₂ O ₅
Formula weight	634.20	1243.23	1272.07	579.54	583.53
Temperature (K)	293(2)	100(2)	150(2)	150(2)	150(2)
Wavelength, (Å)	0.71073	0.71073	0.71073	0.71073	0.71075
Crystal system	Triclinic	Monoclinic	Monoclinic	Tetragonal	Tetragonal
Space group	P $\bar{1}$	C2/c	C2/c	I4 ₁	I4 ₁
a (Å)	7.8156(8)	31.05(14)	31.01(7)	20.2631(3)	20.184(4)
b (Å)	10.315(2)	9.83(4)	9.72(2)	--	20.184(4)
c (Å)	20.747(2)	20.58(9)	20.78(2)	13.8155(5)	13.719(3)
α (°)	101.27(1)	--	--	--	--
β (°)	100.209(8)	101.19(8)	101.99(3)	--	--
γ (°)	97.11(1)	--	--	--	--
Volume (Å ³)	1592.5(4)	6161(46)	6126(24)	5672.6(2)	5589(2)
Z	2	4	4	8	8
D(calcd), Mg/m ³	1.323	1.340	1.379	1.357	1.387
abs coeff, mm ⁻¹	0.732	0.474	0.850	0.509	0.658
Cryst. size, mm ³	0.40 x 0.20 x 0.17	0.22 x 0.16 x 0.07	0.21 x 0.09 x 0.04	0.40 x 0.30 x 0.30	0.03 x 0.08 x 0.32
θ range	2.05 to 24.96°	3.02 to 25°	2 to 25°	1.78 to 27.53°	2.3 to 31.3
Goodness-of-fit on F ²	1.029	1.057	1.191	1.019	0.852
R ₁ [$I > 2\sigma(I)$]	0.0467	0.0577	0.0479	0.0273	0.0334
R ₂ [$I > 2\sigma(I)$]	0.1188	0.1522	0.1346	0.0614	0.0886

Compound	6	8	9	10	11*
Identification code	RM116b	RM135a	RK1_163	RM130	RK1_195
Formula	C ₃₂ H ₃₂ CuN ₂ O ₅	C ₄₂ H ₅₄ N ₂ O ₄ Zn	C ₂₃ H ₂₆ MnN ₂ O ₅	C ₄₆ H ₅₀ N ₄ O ₉ SZn ₂	C ₃₄ H ₂₈ N ₂ O ₈ P ₂ Zn
Formula weight	588.14	716.24	465.40	965.70	719.89
Temperature (K)	293(2)	293(2)	150(2)	293(2)	150(2)
Wavelength, (Å)	0.71073	0.71073	0.71075	0.71073	0.71075
Crystal system	Tetragonal	Monoclinic	Monoclinic	Monoclinic	Monoclinic
Space group	I4 ₁	C2/m	P2 ₁ /c	C2/c	C2/c
a (Å)	20.5720(8)	12.0429(9)	13.211(8)	28.2040(18)	22.74(12)
b (Å)	20.572(1)	11.3433(5)	11.690(7)	11.4950(15)	28.36(13)
c (Å)	13.725(2)	14.8837(7)	14.445(9)	15.0420(9)	10.39(5)
α (°)	--	--	--	--	--
β (°)	--	98.784(5)	99.84(1)	114.001(5)	101.66(8)
γ (°)	--	--	--	--	--
Volume (Å ³)	5809.0(1)	2009.4(2)	2198(2)	4455.0(7)	6562(56)
Z	8	2	4	4	8
D(calcd), Mg/m ³	1.345	1.184	1.406	1.440	1.458
abs coeff, mm ⁻¹	0.795	0.652	0.637	1.184	0.901
Cryst. size, mm ³	0.35 x 0.2 x 0.15	0.35 x 0.20 x 0.20	0.32 x 0.06 x 0.02	0.15 x 0.10 x 0.10	0.39 x 0.10 x 0.03
θ range	1.40 to 24.98°	1.38 to 24.97	2.3 to 31.3	1.94 to 24.99	2.3 to 31.3
Goodness-of-fit on F ²	1.023	1.064	1.194	1.044	1.310
R ₁ [$I > 2\sigma(I)$]	0.0432	0.0383	0.0814	0.0321	0.1326
R ₂ [$I > 2\sigma(I)$]	0.0910	0.1023	0.1557	0.0793	0.3206

* Poor quality crystals-repeated attempts failed to improve the diffraction quality (R₁ [$I > 2\sigma(I)$] = 0.1326 (11)).

used as the N,N'-donor (in place of 1,10-phen), the role of the substituted acid is reversed and hence they become strictly chelating bidentate ligands. Since 4,4'-bpy bridges the adjacent octahedral metal ions in trans fashion a highly linear polymer is isolated (path b; Scheme 4). Switch over from carboxylate to a diaryl phosphate offers two types of bridging ligands at metal

(viz. 4,4'-bpy and dpp⁻) and hence only a 2-D polymeric sheet is isolated (path c; Scheme 4). Thus by tuning both carboxylate (or phosphate) and N,N'-donor ligand, diverse polymeric compounds can be designed.

UV-visible studies

The UV-visible spectrum of **1** shows strong absorption at 290 nm in methanol and 292 nm in dimethylsulfoxide. Complex **2** also shows strong absorption at 294 nm in methanol and 298 nm in dimethylsulfoxide. These transitions are due to the π - π^* transitions of the aromatic moieties present in the complex. No major solvent effect has been observed. Similarly the UV-visible measurements have been carried out for the complexes **3**, **4** and **6-9** in methanol and DMSO and listed in Table 2. The complex **7** shows a weak absorption at 692 nm which may attributed to a metal to ligand charge transfer (MLCT) transition. Strong absorption band observed around 210 and 240 nm for complexes **9** and **10** in methanol may be due to the two different types of π - π^* transitions of the aromatic moieties present in the complex.

Table 2 UV-visible data's for complexes **1-9** in methanol and dimethylsulfoxide.

Complex	λ_{\max} (nm)	λ_{\max} (nm)
	(ϵ , Lmol ⁻¹ cm ⁻¹) in methanol	(ϵ , Lmol ⁻¹ cm ⁻¹) in DMSO
1	290 (3300)	292 (3310)
2	294 (9020)	298 (7190)
3	292 (8800)	294 (5600)
4	--	298 (3400)
6	292 (10700)	296 (58700)
7	296 (7370) 692 (74)	274 (16900) 688 (21)
8	288 (1600)	290 (10200)
9	--	212 (43571) 245 (220342)
10	210 (853903) 238 (676129)	--

Thermo gravimetric analysis

The thermal behavior of all the new compounds **1-11** have been probed by TGA by heating the samples at a rate of 10°C/min. Few representative TGA traces are shown in Fig. 14. The complex **1** exhibits first weight loss at around 297 °C (2%) due to loss of one methanol solvent molecule. The second weight loss observed in the range 297-563 °C (63%) due to loss of organic moiety (tbba and phen) from the complex. The TGA curve of dimeric complex **2** shows the first weight loss around 297 °C (7%) due to loss of solvent molecule. The second weight loss is observed in the temperature range 297-526 °C (74%) due to loss of all organic moiety (tbba and phen) from the complex. The TGA curve of polymer **3** shows the first weight loss at 232 °C corresponding to the loss of one coordinated water molecule. The second and third weight loss that is observed in the range between 232-448 °C (60%) and 448-816 °C (7%) is due to the loss of organic moiety of the complex. Similarly, the polymers **4-7** also show first weight loss at 215 °C due to loss of one coordinated water molecule. The second weight loss in the range 215-818 °C (67%) is due to the loss of organic moiety of the complexes. The TGA of linear polymer **8** shows an initial weight loss in the range 206-274 °C (21%) due to the loss of one 4,4'-bpy unit from the complex. The rail-road like polymer **9** shows

first weight loss at 200 °C (7.5%) due to loss of one acetate unit from the complex, where the second weight loss in the range 196-352 °C (38%) due to the loss of two acid molecules. The third weight loss observed at 484 °C (35 %) due to loss remaining organic units of the complex. The TGA curve of **10** also shows similar types of weight losses like **9**. The compound **11** shows weight loss in the range 200-600 °C due to loss of all organic moieties.

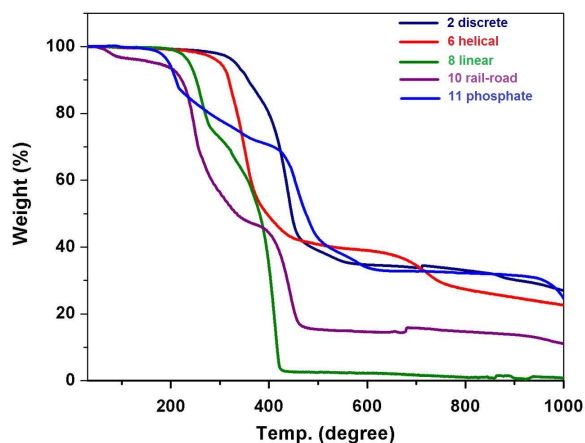


Fig. 14 TGA plot for complexes **2**, **6**, **8**, **9** and **11**.

Conclusion

A series of transition metal benzoates which are having different geometry and coordination modes for the carboxylate have been synthesized from the reaction of metal acetates with aromatic carboxylic acids having different substitutions on the aryl ring and various N-donors. By utilizing the nucleophilic subunits as tunable components of the overall framework instead of merely 'spacers', we are able to change a discrete system to infinite helix polymers and 1-D polymeric systems. The overall crystal-topology of the resulting solid state assembly is found to be highly dependent upon these auxiliary forces, and experiments show that future predictability may be possible with further understanding. The interesting results of 1-D and 2D metallophosphates from various N-donors are currently under investigations.

Experimental Section

Materials and Methods. Manganese acetate, cobalt acetate, zinc acetate, copper acetate, 4,4'-bipyridine (Aldrich), 1,10-phenanthroline (Aldrich), 2,4,6-triisopropylbenzoic acid (Lancaster), 4-tert-butylbenzoic acid (Lancaster), 2,4,6-trimethylbenzoic acid (Lancaster) and diphenylphosphate (Lancaster) have been procured from commercial sources and used as received. Solvents (methanol, acetonitrile and dimethyl sulfoxide) have been purified and dried by employing standard procedures.¹⁵ All the starting materials and the products have been found to be stable towards moisture and air, and hence no specific precaution has been taken to rigorously exclude air.

Melting points have been measured in glass capillaries and are reported uncorrected. Microanalyses have been performed on a Thermo Finnigan (FLASH EA 1112) or a Carlo Erba 1106 microanalyzer. Infrared spectra have been recorded on a Bruker Alpha-P Fourier transform spectrometer and Perkin Elmer FT-IR spectrometer as KBr diluted discs. The ^1H NMR spectra have been recorded on a Bruker Advance DPX-250 spectrometer using $(\text{CH}_3)_4\text{Si}$ as the internal standard. EPR spectral studies have been carried out on a Varian (E-line Century series E-112) spectrometer with 100 kHz field modulations. The magnetic field is calibrated with a proton resonance meter and tetracyanoethylene radical ($g = 2.0077$) as reference. Magnetic measurements have been done on a CAHN electrobalance 7550 model sample magnetometer. Thermal studies have been carried out on a Perkin Elmer Pyris thermal analysis system under nitrogen flow with a heating rate of $10\text{ }^\circ\text{C min}^{-1}$.

General Procedure for complexes. Metal acetate is dissolved in methanol. To this, a solution of N-donors (AL^1/AL^2) in methanol was added. The solution of substituted benzoic acids ($\text{L}^1\text{H}/\text{L}^2\text{H}/\text{L}^3\text{H}$) in methanol was added into the reaction mixture and allowed to stir at RT for 15 min. The mixture was heated using water bath until the solution became clear. The clear solution was layered on a suitable solvent in a beaker and kept for crystallization at RT.

[Cu(L¹)₂(AL¹)(H₂O)](H₂O) (1). Blue colored needles of **1** have been obtained from a mixture of $\text{Cu}(\text{OAc})_2 \cdot 2\text{H}_2\text{O}$ (0.5 mmol, 0.10 g), AL^1 (1 mmol, 0.180 g) and L^1H (1 mmol, 0.1782 g) in methanol/ $\text{CH}_3\text{CN}/\text{DMSO}$ mixture. Yield: 0.27 g (~85% based on Cu). M.p.: 220-222 $^\circ\text{C}$. Elemental Anal. Calcd. for $\text{C}_{34}\text{H}_{34}\text{CuN}_2\text{O}_4$ (%): C, 68.27; H, 5.73; N, 4.68. Found: C, 67.74; H, 5.88; N, 4.37. FT-IR data (KBr, cm^{-1}): 3526(m), 3052(w), 2967(s), 2875(m), 1604(s), 1525(m), 1433(m), 1381(s), 12699(w), 1111(m), 867(s), 788(s). UV-vis (CH_3OH): 296 nm, $\epsilon = 7370\text{ Lmol}^{-1}\text{cm}^{-1}$, $\lambda = 692\text{ nm}$, $\epsilon = 74\text{ Lmol}^{-1}\text{cm}^{-1}$; (THF): 238 nm, $\epsilon = 39,500\text{ Lmol}^{-1}\text{cm}^{-1}$, $\lambda = 660\text{ nm}$, $\epsilon = 22.9\text{ Lmol}^{-1}\text{cm}^{-1}$; (DMSO): $\lambda = 274\text{ nm}$, $\epsilon = 169,00\text{ Lmol}^{-1}\text{cm}^{-1}$, $\lambda = 688\text{ nm}$, $\epsilon = 20.5\text{ Lmol}^{-1}\text{cm}^{-1}$. TGA: Temperature range $^\circ\text{C}$ (weight loss): 29-215 $^\circ\text{C}$ (3%); 215-818 $^\circ\text{C}$ (67%).

[Mn(L¹)₂(AL¹)₂(2CH₃OH) (2). Yellow colored needles of **2** have been obtained from the reaction of $\text{Mn}(\text{OAc})_2 \cdot 6\text{H}_2\text{O}$ (0.25 mmol, 0.0613 g), AL^1 (0.5 mmol, 0.09 g) and L^1H (0.5 mmol, 0.0891 g) in methanol/DMSO solvent mixture. Yield: 0.13 g (~86% based on Mn). M.p.: > 300 $^\circ\text{C}$. Elemental Anal. Calcd. for $\text{C}_{70}\text{H}_{76}\text{Mn}_2\text{N}_4\text{O}_{10}$ (%): C, 67.63; H, 6.16; N, 4.51. Found: C, 67.79; H, 6.01; N, 5.38. FT-IR data (KBr, cm^{-1}): 3063(m), 2971(s), 2905 (s), 2875 (s), 1932 (w), 1617(s), 1566(s), 1420(s, br), 1270(s), 1107(m), 1026(s), 802(s). UV-vis (CH_3OH): $\lambda = 290\text{ nm}$, $\epsilon = 3,300\text{ Lmol}^{-1}\text{cm}^{-1}$; (DMSO): $\lambda = 292\text{ nm}$, $\epsilon = 3,310\text{ Lmol}^{-1}\text{cm}^{-1}$ (compound is insoluble in THF). TGA: Temperature range $^\circ\text{C}$ (weight loss): 30-297 $^\circ\text{C}$ (3%); 297-563 $^\circ\text{C}$ (62%).

[Zn(L¹)₂(AL¹)₂(2CH₃OH) (3). Colorless block-like single crystals of **3** have been obtained from the reaction of $\text{Zn}(\text{OAc})_2 \cdot 2\text{H}_2\text{O}$ (0.5 mmol, 0.11 g), AL^1 (1 mmol, 0.180 g) and L^1H (1 mmol, 0.1782 g) in a methanol/DMSO mixture. Yield: 0.24 g (~79% based on Zn). M.p.: > 270 $^\circ\text{C}$. Elemental Anal. Calcd. for $\text{C}_{68}\text{H}_{68}\text{N}_4\text{O}_8\text{Zn}_2$ (%): C, 68.05; H, 5.71; N, 4.67.

Found: C, 67.72; H, 6.20; N, 4.43. FT-IR data (KBr, cm^{-1}): 3368(w), 3065(m), 2960(s), 2874(m), 1636(s), 1570(m), 1432(s), 1353(s), 1109(m), 852(s), 793(s), 727(s). ^1H NMR (400 MHz, $\text{DMSO}-d_6$) (ppm): δ 9.16 (b, 2H, H^1 , phen), 8.87 (d, $J = 8.08\text{ Hz}$, 2H, H^3 , phen), 8.24 (s, 2H, H^4 , phen), 8.07 (b, 2H, H^2 , phen), 7.80 (d, $J = 7.92\text{ Hz}$, 4H, H^5 , acid), 7.35 (d, $J = 7.96\text{ Hz}$, 4H, H^5 , acid), and 1.24 (s, 9H, CH_3 -tertbutyl of acid). UV-vis (CH_3OH): $\lambda = 294\text{ nm}$, $\epsilon = 9,020\text{ Lmol}^{-1}\text{cm}^{-1}$; (DMSO): $\lambda = 298\text{ nm}$, $\epsilon = 7,190\text{ Lmol}^{-1}\text{cm}^{-1}$. TGA: Temperature range $^\circ\text{C}$ (weight loss): 30-296 $^\circ\text{C}$ (7%); 296-344 $^\circ\text{C}$ (17%); 344-462 $^\circ\text{C}$ (48%); 462-526 $^\circ\text{C}$ (7%).

[Mn(L²)₂(AL¹)(H₂O)]_n (4). Yellow colored needles of **4** have been obtained from the reaction of $\text{Mn}(\text{OAc})_2 \cdot 6\text{H}_2\text{O}$ (0.25 mmol, 0.0613 g), AL^1 (0.5 mmol, 0.09 g) and L^2H (0.5 mmol, 0.0821 g) in a solvent mixture consisting of methanol, CH_3CN and DMSO. Yield: 0.13 g (~87% based on Mn). M.p.: 186-188 $^\circ\text{C}$. Elemental Anal. Calcd. for $\text{C}_{32}\text{H}_{32}\text{MnN}_2\text{O}_5$ (%): C, 66.32; H, 5.57; N, 4.83. Found: C, 65.41; H, 5.45; N, 5.10. FT-IR data (KBr, cm^{-1}): 3307(m), 3063(m), 3012(m), 2961(m), 2931(m), 2737(m), 1571(s), 1439(s), 1398(s), 1184(s), 1118(s), 1031(s), 858(s), 802(s), 741(s), 644(s), 599(s). UV-vis (CH_3OH): $\lambda = 292\text{ nm}$, $\epsilon = 8,800\text{ Lmol}^{-1}\text{cm}^{-1}$; (THF): $\lambda = 292\text{ nm}$, $\epsilon = 61,00\text{ Lmol}^{-1}\text{cm}^{-1}$; (DMSO): $\lambda = 294\text{ nm}$, $\epsilon = 56,00\text{ Lmol}^{-1}\text{cm}^{-1}$. TGA: Temperature range $^\circ\text{C}$ (weight loss): 30-232 $^\circ\text{C}$ (3%); 232-448 $^\circ\text{C}$ (60%); 448-816 $^\circ\text{C}$ (6%).

[Co(L²)₂(AL¹)(H₂O)]_n (5). Orange colored crystals of **5** have been obtained from the reaction of $\text{Co}(\text{OAc})_2 \cdot 6\text{H}_2\text{O}$ (0.25 mmol, 0.071 g), AL^1 (0.5 mmol, 0.09 g) and L^2H (0.5 mmol, 0.0821 g) in a solvent mixture consisting of methanol and DMSO. Yield: 0.119 g (~82% based on Mn). Elemental Anal. Calcd. for $\text{C}_{32}\text{H}_{32}\text{CoN}_2\text{O}_5$ (%): C, 65.86; H, 5.53; N, 4.80. Found: C, 65.62; H, 5.32; N, 4.72. FT-IR data (KBr, cm^{-1}): 3301-63(br), 3007(m), 2942(m), 2925(m), 1583(s), 1436(s), 1402 (s), 1171(s), 858(s).

[Cu(L²)₂(AL¹)(H₂O)]_n (6). Blue colored needles of **6** have been obtained from the reaction of $\text{Cu}(\text{OAc})_2 \cdot 2\text{H}_2\text{O}$ (0.25 mmol, 0.05 g), AL^1 (0.5 mmol, 0.0901 g) and L^2H (0.5 mmol, 0.0821 g) in methanol/ $\text{CH}_3\text{CN}/\text{DMSO}$ solvent mixture. Yield: 0.12 g (~78% based on Cu). M.p.: 140 $^\circ\text{C}$. Elemental Anal. Calcd. for $\text{C}_{32}\text{H}_{32}\text{CuN}_2\text{O}_5$ (%): C, 65.35; H, 5.48; N, 4.76. Found: C, 65.46; H, 4.85; N, 4.77. FT-IR data (KBr, cm^{-1}): 3058-2865(br), 1566(br), 1444(s), 1398(br), 1189(m), 1118(m), 1047(w, br), 980(w, br), 853(s), 807(s), 726(s), 598(m). UV-vis (THF): $\lambda = 302\text{ nm}$, $\epsilon = 5,068\text{ Lmol}^{-1}\text{cm}^{-1}$; (DMSO): $\lambda = 298\text{ nm}$, $\epsilon = 3,400\text{ Lmol}^{-1}\text{cm}^{-1}$. TGA: Temperature range $^\circ\text{C}$ (weight loss): 29-215 $^\circ\text{C}$ (3%); 215-818 $^\circ\text{C}$ (67%).

[Zn(L²)₂(AL¹)(H₂O)]_n (7). Colorless block-like single crystals of **7** have been obtained from the reaction of $\text{Zn}(\text{OAc})_2 \cdot 2\text{H}_2\text{O}$ (0.25 mmol, 0.055 g), AL^1 (0.5mmol, 0.0901 g) and L^2H (0.5 mmol, 0.0821 g) in methanol/ $\text{CH}_3\text{CN}/\text{DMSO}$ solvent mixture. Yield: 0.12 g (~81% based on Zn). M.p.: 140 $^\circ\text{C}$. Elemental Anal. Calcd. for $\text{C}_{32}\text{H}_{32}\text{ZnN}_2\text{O}_5$ (%): C, 65.14; H, 5.47; N, 4.75. Found: C, 65.65; H, 5.43; N, 4.46. FT-IR data (KBr, cm^{-1}): 3262(m), 3068(m), 3007(m), 2966(m), 2931(m), 15869(s), 1438(s), 1382(s), 1189(s), 1123(s), 1036(s), 858(s), 807(s), 735(s), 644(m), 613(s). UV-vis (CH_3OH): $\lambda = 292\text{ nm}$, $\epsilon = 10,700\text{ Lmol}^{-1}\text{cm}^{-1}$; (THF): $\lambda = 294\text{ nm}$, $\epsilon = 140,00\text{ Lmol}^{-1}\text{cm}^{-1}$; (DMSO): $\lambda = 296\text{ nm}$, $\epsilon = 58,700\text{ Lmol}^{-1}\text{cm}^{-1}$. ^1H NMR (400

MHz, DMSO-*d*₆) (ppm): δ 9.19 (b, 2H, H¹, phen), 8.89 (d, *J* = 8.32 Hz, 2H, H³, phen), 8.26 (s, 2H, H⁴, phen), 8.10 (m, 2H, H², phen), 7.82 (d, *J* = 8.28 Hz, 4H, H⁵, acid), 7.36 (d, *J* = 8.28 Hz, 4H, H^{5'}, acid), and 1.3 (s, 9H, CH₃-acid). UV-vis (CH₃OH): λ = 292 nm, ε = 10,700 Lmol⁻¹cm⁻¹ (THF): λ = 294 nm, ε = 140,00 Lmol⁻¹cm⁻¹. (DMSO): λ = 296 nm, ε = 58,700 Lmol⁻¹cm⁻¹. TGA: Temperature range °C (weight loss): 29-252 °C (3%); 252-816 °C (58%). TGA: Temperature range °C (weight loss): 29-215 °C (3%); 215-818 °C (67%).

[Zn(L³)₂(AL²)_n (8). Cubic colorless single crystals of **8** have been obtained from the reaction of Zn(OAc)₂·2H₂O (0.25 mmol, 0.0549 g), AL² (0.5 mmol, 0.08 g) and L³H (0.5 mmol, 0.124 g) in methanol/DMSO solvent mixture. Yield: 0.15 g (~83% based on Zn). M.p.: 262 °C. Elemental Anal. Calcd. for C₄₂H₅₄N₂O₄Zn (%): C, 70.42; H, 7.60; N, 3.91. Found: C, 70.31; H, 7.89; N, 3.63. FT-IR data (KBr, cm⁻¹): 3500(w, br), 3204(w, br), 3065(m), 2960(s, br), 1618(s), 1558(s), 1525(s), 1460(m), 1321(m), 1229(m), 1117(m), 1071(m), 874(s), 828(s), 643(s). UV-vis (CH₃OH): λ = 288 nm, ε = 1,600 Lmol⁻¹cm⁻¹; (THF): λ = 290 nm, ε = 10,200 Lmol⁻¹cm⁻¹; (DMSO): λ = 290 nm, ε = 2,260 Lmol⁻¹cm⁻¹. ¹H NMR (400 MHz, DMSO-*d*₆) (ppm): δ 8.74 (d, *J* = 5.88 Hz, 4H, H^a, bpy), 7.88 (dd, *J* = 4.6 Hz, 4H, H^b, bpy), 6.93 (s, 4H, H¹, acid), 3.13 (m, 2H, H², isopropyl, acid), 2.86 (m, 2H, H², isopropyl, acid), 1.19 (d, *J* = 6.92 Hz, H³, CH₃-isopropyl, acid), and 1.16 (d, *J* = 6.88 Hz, H³, CH₃-isopropyl, acid). UV-vis (CH₃OH): λ = 288 nm, ε = 1,600 Lmol⁻¹cm⁻¹; (THF): λ = 290 nm, ε = 10,200 Lmol⁻¹cm⁻¹; (DMSO): λ = 290 nm, ε = 2,260 Lmol⁻¹cm⁻¹. TGA: Temperature range °C (weight loss): 29-207 °C (0.5%); 207-274 °C (21%); 274-430 °C (75.5%).

[Mn(L²)(OAc)(AL²)_n (9). Yellow colored needles of **9** have been obtained from the reaction of Mn(OAc)₂·6H₂O (0.123 g, 0.5 mmol), AL² (0.08 g, 0.5 mmol) and L²H (0.164 g, 1 mmol) in methanol/DMSO solvent mixture. Yield: 0.106g (42.6%). Anal. Calcd. for C₂₄H₃₀N₂O₆Mn (%): C, 57.95, H, 6.08, N, 5.63. Found: C, 57.35, H, 5.56, N, 5.80. IR (as KBr disc, cm⁻¹): 2954(s), 2855(s), 1612(s), 1419(s), 1418(s), 1377(s), 1365(s), 1221(s), 1179(s), 1173(w), 814(s). TGA: Temperature range °C (weight loss): 29-196 °C (7%); 196-352 °C (45%); 352-484 °C (37%).

[Zn(L²)(OAc)(AL²)_n (10). Colorless needles of **10** have been obtained from the reaction of Zn(OAc)₂·2H₂O (0.055 g, 0.25 mmol), AL² (0.04 g, 0.25 mmol) and L²H (0.082 g, 0.5 mmol) in methanol/DMSO solvent mixture. Yield: 0.128g (72%) M.p. 255 °C. Anal. Calcd. for C₂₃H₂₆N₂O₅Zn (%): C, 58.05, H, 5.51, N, 5.89. Found: C, 58.43, H, 5.49, N, 6.01. IR (as KBr disc, cm⁻¹): 2954(s), 2855(s), 1612(s), 1419(s), 1418(s), 1377(s), 1365(s), 1221(s), 1179(s), 1173(w), 814(s). ¹H NMR (400 MHz, DMSO-*d*₆) (ppm): δ 8.73 (b, 4H, H^a, bpy), 7.86 (d, *J* = 5.96 Hz, 4H, H^b, bpy), 6.76 (s, 2H, H¹, acid), 2.53 (s, 6H, acid (CH₃-acetate)), 2.20 (s, 6H, acid, -CH₃) and 1.82 (s, 3H, -CH₃). UV-vis (CH₃OH): λ = 210 nm, ε = 853903 L mol⁻¹cm⁻¹, λ = 238 nm, ε = 676,129 L mol⁻¹cm⁻¹. TGA: Temperature range °C (weight loss): 29-226 °C (35%); 226-786 °C (45%).

[Zn(L⁴)₂(AL²)_n (11). A methanol solution of Zn(OAc)₂·2H₂O (0.055 g, 0.25 mmol) and AL² (0.040 g, 0.25 mmol) stirred at RT for 1h and L⁴H (125 mg, 0.5 mmol) was added to the reaction mixture and allowed to continuously stir for 20 min. The precipitate was separated by filtration. The clear

solution was kept for crystallization with 5 mL DMSO solution. Colorless needles of **11** have been obtained after 1 week. Yield: 0.109 g (60%). Anal. Calcd. for C₃₄H₂₈N₂O₈P₂Zn (%): C, 56.72, H, 3.92, N, 3.89. Found: C, 58.43, H, 5.49, N, 6.01. IR (as KBr disc, cm⁻¹): 2959(s), 1596(s), 1579(s), 1473(s), 1439(s), 1315(s), 1195(s), 1091(b), 759(s), 560(s). ¹H NMR (400 MHz, DMSO-*d*₆) (ppm): δ 8.73 (dd, 4H, H^a, bpy), 7.84 (dd, 4H, H^b, bpy), 7.25 (t, 4H, H², dpp), 7.15 (d, 4H, H¹, dpp) and 6.99 (t, 2H, H³, dpp). ³¹P NMR (DMSO-*d*₆, 100 MHz): δ -12.56 ppm.

X-ray diffraction Studies. The intensity data collection for compounds **1**, **8** and **10** have been carried out on a Nonius MACH3 four circle diffractometer while data measurement for compounds **4** and **6** have been carried out on an STOE-AED2 diffractometer. The intensity data for complexes **2**, **3**, **5**, **9** and **11** have been obtained on a Rigaku Saturn 724+ CCD diffractometer. The unit cell dimensions have been determined using well-centered and well-separated high angle reflections. Intensity data collection and cell determination protocols have been carried out using a graphite-mono chromatized Mo Kα radiation (λ = 0.71073 Å) in each case. The resultant intensity data have been corrected for Lorentz polarization and absorption effects. All calculations have been carried out using WinGX. The structure solution is achieved by direct methods as implemented in SIR-92. The final refinement of the structure has been carried using full least-squares methods on F² using SHELXL-97.¹⁶The positions of hydrogen atoms have either been located in the successive difference maps or geometrically fixed and refined using a riding model. All non-hydrogen atoms have been refined anisotropically. Hydrogen bond parameters in each of the compounds have been calculated using PARST.¹⁶ The crystal data for compounds **1-6** and **8-10** are listed in Table 1.

Acknowledgement

This work was supported by CSIR New Delhi. RM thanks DAE for a DAE-BRNS Outstanding Investigator Award, which enable the purchase of a single crystal diffractometer.

Notes and references

^aDepartment of Chemistry, Indian Institute of Technology Bombay, Powai, Mumbai 400 076, India. Fax: +91 22 2576 7152; Tel: +91 22 2576 7163; E-mail: rmv@chem.iitb.ac.in

^bDepartment of Chemistry, Howard University, Washington, DC 20059, USA.

† Electronic Supplementary Information (ESI) available: ¹H NMR, ¹³C NMR, ESI-MS spectra and PXRD pattern. Selected bond lengths and angles of compounds **1-11** and comparison with the related compounds. Crystallographic data of **1-6** and **8-10**. CCDC 993872-993880 and 1010743. For ESI and crystallographic data in CIF or other electronic format see DOI: 10.1039/b000000x.

References

- (1) (a) J. M. Lehn, *Supramolecular Chemistry, Concepts, Perspectives*, VCH, Weinheim, 1995; (b) H. C. Zhou, J. R. Long and O. M. Yaghi, *Chem. Rev.* 2012, **112**, 673; (c) T. R. Cook, Y. R.; Zheng and P. J. Stang, *Chem. Rev.* 2013, **113**, 734; (d) M. Dinca and J. R. Long, *Angew. Chem. Int. Ed.*, 2008, **47**, 6766; (e) M. Eddaoudi, D. B. Moler, H. Li, B. Chen, T. M. Reineke, M. O'Keeffe and O. M. Yaghi, *Acc. Chem. Res.* 2001, **34**, 319; (f) G. B. Deacon and R. Phillips, *J. Coord. Chem. Rev.* 1980, **33**, 227.

- (2) (a) D. J. Tranchemontagne, D. S. Park, H. Furukawa, J. Eckert, C. B. Knobler and O. M. Yaghi, *J. Phy. Chem. C* 2012, **116**, 13143; (b) C. N. R. Rao, S. Natarajan and R. Vaidhyanathan, *Angew. Chem. Int. Ed.*, 2004, **43**, 1466; (c) G. Prabusankar and R. Murugavel, *Organometallics* 2004, **23**, 5644; (d) R. Murugavel and S. Banerjee, *Inorg. Chem. Commun.* 2003, **6**, 810; (e) R. Murugavel, D. Krishnamurthy and M. Sathiyendiran, *Dalton Trans.* 2002, 34.
- (3) (a) H. Deng, S. Grunder, K. E. Cordova, C. Valente, H. Furukawa, H. Hmadeh, F. Gándara, A. C. Whalley, Z. Liu, S. Asahina, H. Kazumori, M. O'Keeffe, O. Terasaki, J. F. Stoddart and O. M. Yaghi, *Science* 2012, **336**, 1018; (b) R. Nayuk, D. Zacher, R. Schweins, C. Wiktor, R. A. Fischer, G. van Tendeloo and K. Huber, *J. Phy. Chem. C* 2012, **116**, 6127; (c) N. Palanisami and R. Murugavel, *Inorg. Chim. Acta*. 2011, **365**, 430; (d) N. Palanisami, G. Prabusankar and R. Murugavel, *Inorg. Chem. Commun.* 2006, **9**, 1002; (e) R. Murugavel, K. Baheti and G. Anantharaman, *Inorg. Chem.* 2001, **40**, 6870; (f) R. Murugavel, V. V. Karambelkar, G. Anantharaman and M. G. Walawalkar, *Inorg. Chem.* 2000, **39**, 1381; (g) R. Murugavel, G. Anantharaman, D. Krishnamurthy, M. Sathiyendiran and M. G. Walawalkar, *Proc. Ind. Acad. Sci. (Chem. Sci.)*, 2000, **112**, 273.
- (4) (a) P. K. Yadav, N. Kumari, P. Pachfule, R. Banerjee and L. Mishra, *Cryst. Growth Des.* 2012, **12**, 5311; (b) W. Morris, B. Voloskiy, S. Demir, F. Gándara, P. L. McGrier, H. Furukawa, D. Cascio, J. F. Stoddart and O. M. Yaghi, *Inorg. Chem.* 2012, **51**, 6443; (d) Y. Yan, X. Lin, S. Yang, A. J. Blake, A. Dailly, N. R. Champness, P. Hubberstey and M. Schroder, *Chem. Commun.* 2009, 1025; (e) E. Hough, L. K. Hansen, B. Birknes, K. Jynge, S. Hansen, A. Hardvik, C. Little, E. Dodson and Z. Derewenda, *Nature* 1989, **338**, 357; (f) P. Lemoine, B. Viossat, G. Morgant, F. T. Greenaway, A. Tomas, N-H. Dung and J. R. J. Sorenson, *Inorg. Biochem.* 2002, **89**, 18; (g) X-M. Chen, Z-T. Xu, X-L. Yu and T. C. W. Mak, *Polyhedron* 1994, **13**, 2079; (h) X-M. Chen and Y-X. Tong, *Inorg. Chem.* 1994, **33**, 4586; (i) X-M. Chen, T-U. Xu, T. C. W. Mak, *Polyhedron* 1994, **13**, 3329.
- (5) (a) P. Pachfule and R. Banerjee, *Cryst. Growth Des.* 2012, **12**, 4292; (b) S. M. Vickers, P. D. Frischmann and M. J. MacLachlan, *Inorg. Chem.* 2011, **50**, 2957; (c) S. Zhang, J. Lan, Z. Mao, R. Xie and J. You, *Cryst. Growth Des.* 2008, **8**, 3134; (d) M. Fujita, Y. J. Kwon, M. Miyazawa and K. Ogura, *J. Chem. Soc. Chem. Commun.*, 1994, 1977; (e) H. Sigel and R. B. Martin, *Chem. Soc. Rev.* 1994, **23**, 83; (f) M. F. Summers, *Coord. Chem. Rev.* 1988, **86**, 43.
- (6) (a) M. Schweiger, S. R. Seidel, A. M. Arif and P. J. Stang, *Inorg. Chem.* 2002, **41**, 2556; (b) J. C. Noveron, M. S. Lah, R. E. D. Sesto, A. M. Arif, J. S. Miller and P. J. Stang, *J. Am. Chem. Soc.* 2002, **124**, 6613; (c) F. M. Tabellion, S. R. Seidel, A. M. Arif and P. J. Stang, *J. Am. Chem. Soc.* 2001, **123**, 11982; (d) C. J. Kuehl, F. M. Tabellion, A. M. Arif and P. J. Stang, *Organometallics* 2001, **20**, 1956; (e) S. D. Huang, C. J. Kuehl and P. J. Stang, *J. Am. Chem. Soc.* 2001, **123**, 9634.
- (7) (a) C. H. Yoon, M. J. Zaworotko, B. Moulton and K. W. Jung, *Org. Lett.* 2001, **3**, 3539; (b) M. D. Fryzuk, P. B. Duval, S. S. H. Mao, M. J. Zaworotko and L. R. MacGullivray, *J. Am. Chem. Soc.* 1999, **121**, 2478; (c) S. A. Bourne, J. Lu, A. Mondal, B. Moulton and M. J. Zaworotko, *Angew. Chem. Int. Ed.* 2001, **40**, 2111; (d) B. Rather, B. Moulton, R. D. B. Walsh and M. J. Zaworotko, *Chem. Commun.* 2002, 694; (e) L. R. MacGullivray, S. Subramanian, M. J. Zaworotko and K. Biradha, *Inorg. Chem.* 1999, **38**, 5078.
- (8) (a) D. Braga, L. Maini, F. Grepioni, G. Cojazzi and D. Emiliani, *Chem. Commun.* 2001, 2272; (b) D. Braga, L. Maini and F. Grepioni, *J. Organomet. Chem.* 2000, **593**, 101; (c) F. Grepioni, G. Cojazzi, D. Braga, E. Marseglia, L. Scac-cianoce and B. F. G. Johnson, *J. Chem. Soc., Dalton Trans.* 1999, 553; (d) D. Braga, L. Maini, G. Cojazzi and M. Polito, *Chem. Commun.* 1999, 1949; (e) D. Braga, L. Maini, F. Grepioni and M. Polito, *Organometallics* 1999, **18**, 2577; (f) D. Braga, L. Maini and F. Grepioni, *Chem. Commun.* 1999, 937.
- (9) (a) P. Grossham, A. Jouaiti and M. W. Hosseini, *New J. Chem.* 2003, 793; (b) A. Jouaiti, M. W. Hosseini and N. Kyritsakas, *Chem. Commun.* 2003, 472; (c) C. Kaes, A. Katz and M. W. Hosseini, *Chem. Rev.* 2000, **100**, 3553; (d) A. Jouaiti, M. W. Hosseini and N. Kyritsakas, *Chem. Commun.* 2002, 1898; (e) B. Schmaltz, M. W. Hosseini and A. D. Cian, *Chem. Commun.* 2001, 1242.
- (10) (a) W. Morris, B. Voloskiy, S. Demir, F. Gandara, P. L. McGrier, H. Furukawa, D. Cascio, J. F. Stoddart and O. M. Yaghi, *Inorg. Chem.* 2012, **51**, 6443; (b) S. Wan, F. Gandara, A. Asano, H. Furukawa, A. Saeki, S. K. Dey, L. Liao, M. W. Ambrogio, Y. Y. Botros, X. Duan, S. Seki, F. J. Stoddart and O. M. Yaghi, *Chem. Mater.* 2011, **23**, 4094; (c) Y. R. Zheng, Z. Zhao, M. Wang, K. Ghosh, J. B. Pollock, T. R. Cook and P. J. Stang, *J. Am. Chem. Soc.* 2010, **132**, 16873; (d) Z. Zhao, Y. R. Zheng, M. Wang, J. B. Pollock and P. J. Stang, *Inorg. Chem.* 2010, **49**, 8653.
- (11) (a) B-H. Ye, M-L. Tong and X-M. Chen, *Coord. Chem. Rev.* 2005, **249**, 545; (b) F. Marandi, M. Ghadermazi, A. Marandi, I. Pantenburg and G. Meyer, *J. Mol. Struct.* 2011, **1006**, 136.
- (12) (a) P. J. Stang and B. Olenyuk, *Acc. Chem. Res.* 1997, **30**, 502; (b) B. H. Northrop, R. Zheng, K. W. Chi and P. J. Stang, *Acc. Chem. Res.* 2009, **42**, 1554; (c) K. Biradha, M. Sarkar and L. Rajput, *Chem. Commun.* 2006, 4169; (d) R. Pothiraja, M. Sathiyendiran, R. J. Butcher and R. Murugavel, *Inorg. Chem.* 2005, **44**, 6314; (e) R. Pothiraja, M. Sathiyendiran, R. J. Butcher and R. Murugavel, *Inorg. Chem.* 2004, **43**, 7585.
- (13) (a) T. Osuga, T. Murase, K. Ono, Y. Yamauchi and M. Fujita, *J. Am. Chem. Soc.* 2010, **132**, 15553; (b) S. R. Batten and R. Robson, *Angew. Chem., Int. Ed. Engl.*, 1998, **37**, 1460; (c) S. Kitagawa and M. Kondo, *Bull. Chem. Soc. Jpn.* 1998, **71**, 1735.
- (14) (a) R. Chakrabarty, P. S. Mukherjee and P. J. Stang, *Chem. Rev.* 2011, **111**, 6810; (b) D. Gupta, P. Rajakannu, B. Shankar, R. Shanmugam, F. Hussain, B. Sarkar and M. Sathiyendiran, *Dalton Trans.* 2011, **40**, 5433; (c) Y. Yamauchi and M. Fujita, *Chem. Commun.* 2010, **46**, 5897; (d) A. J. Blake, N. R. Champness, P. Hubberstey, W. S. Li, M. A. Withersby and M. Schröder, *Coord. Chem. Rev.* 1999, **183**, 117.
- (15) (a) D. D. Perrin and W. L. F. Armarego, *Purification of Laboratory Chemicals*, 3rd Edn., *Pergamon Press*: 1988; (b) *Vogel's Text Book of Practical Organic Chemistry*, 5th Edn., *Langman Group*: Essex, Harlow, UK, 1989.
- (16) (a) L. J. Farrugia, WinGX, Version: 1.64.05 *J. Appl. Cryst.* 1999, **32**, 837; (b) G. M. Sheldrick, SHELXL-97, Program for Structure Refinement; University of Göttingen, Germany, 1997.
- (17) (a) Y.-L. Zhou, H.-Y. He, Y. Zhang and L.-G. Zhu, *Acta Cryst.* 2003, **E59**, m605; (b) C. Aller, J. Castro, P. Pérez-Lourido, E. Labisbal, J. A. García-Vázquez, *Acta Cryst.* 2002, **C58**, m155; (c) Z.-W. Mao, G. Liehr and R. van Eldik, *J. Am. Chem. Soc.* 2000, **122**, 4839; (d) L. Antolini, L. P. Battaglia, A. B. Corradi, G. Marcotrigiano, L. Meanabue, G. C. Pellacani, M. Saladini and M. Sola, *Inorg. Chem.* 1986, **25**, 2901; (e) M. C. Lim, E. Sinn and R. B. Martin, *Inorg. Chem.* 1976, **15**, 807; (f) L. P. Battaglia, A. C. Bonamartini, S. Ianelli, M. A. Zoroddu, G. Sanna, *J. Chem. Soc., Faraday Trans.*

- 1991, **87**, 3863; (g) X.-F. Chen, P. Cheng, X. Liu, B. Zhao, D.-Z. Liao, S.-P. Yan and Z.-H. Jiang, *Inorg. Chem.* 2001, **40**, 2652; (h) P. Lemonie, B. Viossat, G. Morgant, F. T. Greenaway, A. Tomas, N.-H. Dung and J. R. J. Sorenson, *J. Inorg. Biochem.* 2002, **89**, 18; (i) M. McCann, M. Devereux, C. Cardin and M. Convery *Polyhedron* 1994, **13**, 221; (j) A. C. Fabretti, G. Franchini, P. Zannini, *Inorg. Chim. Acta* 1985, **105**, 187; (k) W.-L. Kwik, K.-P. Ang and H. S.-O. Chan, *J. Chem. Soc., Dalton Trans.* 1986, 2519.
- (18) X. Zhang, C. Fan, W. Wang, C. Chen and Q. Liu, *Acta Cryst.* 2002, **E58**, m688; (b) J. M. S. Skakle, M. R. J. Foreman and M. J. Plater *Acta Cryst.* 2001, **E57**, m373; (c) X. Zhang, C. Feng, W. Wang, C. Chen and Q. Liu, *Acta Cryst.* 2002, **E58**, m360; (d) Y.-Q. Zheng, J.-L. Lin and J. Sun, *Z. Anorg. Allg. Chem.* 2001, **627**, 1059; (e) M. Devereux, M. McCann, V. Leon, M. Geraghty, V. McKee and J. Wikaira, *Polyhedron* 2000, **19**, 1205; (f) X.-M. Chen and Y.-J. Zhu, *Polyhedron* 1994, **13**, 1393; (g) J. Cano, G. De Munno, J. L. Sanz, R. Ruiz, J. Faus, F. Lloret, M. Julve and A. Caneschi, *J. Chem. Soc., Dalton Trans.* 1997, 1915.
- (19) (a) J. Yang, J.-F. Ma and J.-F. Liu, *Acta Cryst.* 2003, **E59**, m324; (b) X.-M. Chen, Z.-T. Xu, X.-L. Yu, *Polyhedron* 1994, **13**, 2079.
- (20) (a) K. O. Kongshaug and H. J. Fjellvag, *Solid State Chem.* 2003, **175**, 182; (b) Y.-Q. Zheng, J.-L. Lin and J.-Y. Jiang, *Z. Kristallogr.-New Cryst. Struct.* 2003, **218**, 229; (c) C.-D. Wu, C.-Z. Lu, D.-M. Wu, H.-H. Zhuang and J.-S. Huang, *Inorg. Chem. Commun.* 2001, **4**, 561; (d) J. Tao, M. -L. Tong, J. -X. Shi, X.-M. Chen and S. W. Ng, *Chem. Commun.* 2000, **20**, 2043; (e) S.-M. Ying, J.-G. Mao, Y.-Q. Sun, H.-Y. Zeng and Z.-C. Dong, *Polyhedron* 2003, **22**, 3097.
- (21) R. Dey, B. Bhattacharya, E. Colacio and D. Ghoshal, *Dalton Trans.*, 2013, **42**, 2094.

30